

Anti-sway system with image sensor for container cranes[†]

Hideki Kawai¹, Young Bok Kim^{2,*} and Yong Woon Choi¹

¹Faculty of Engineering, Soka University, Tokyo, 192-8577, Japan

²Department of Control and Mechanical Engineering, Pukyong National University, Busan, 608-739, Korea

(Manuscript Received August 11, 2008; Revised April 27, 2009; Accepted April 29, 2009)

Abstract

High speed and efficiency are highly important factors in handling cargo at ports. The ability to handle cargo at high speed strongly depends on the anti-sway system employed. However, it is not easy to realize a high-performance anti-sway control system due to a number of problems. High-speed operation of container cranes is continuously required for crane operators who work as cargo handlers at ports. Undesirable motion can lower the work efficiency due to the prolonged strain to which operators are subjected. To overcome this problem, we propose an anti-sway system with an image sensor for container cranes. In this system, the image sensor is used for measuring the motion of the spreader, and the measured data are fed back to the controller in real time. The applied image processing technique is a kind of robust template matching method referred to as vector code correlation (VCC), which was devised in order to consider real environmental conditions. The anti-sway system proposed in this paper is a mass damper type system in which a movable mass is installed on the spreader. The actuator acting on the movable mass applies inertial force to the spreader, which results in suppressing undesirable sway motion. The system is simple and can be easily applied to any crane system. In this regard, the useful features and the performance of the proposed anti-sway system are experimentally verified.

Keywords: Anti-sway control; Container crane; Image sensor; Robust template matching

1. Introduction

One of the exciting application areas for feedback system design involves the protection of civil engineering structures from dynamic loading, such as strong earthquakes, high wind, extreme waves, heavy traffic and highway loading. Buildings and other physical structures, including highway infrastructure, have traditionally relied on their strength and ability to dissipate energy to survive severe dynamic loading. In recent years, the attention of a large number of researchers has been directed toward the use of control and automation for the mitigation of the effects of dynamic loading on such structures [1-3].

The protection of structures is unquestionably a worldwide priority of utmost importance. Such protection can range from reliable operation through comfort to survivability. In this article, we provide a genuine contribution to one of these problem areas, namely, the problem of controlling undesirable sway motion.

Container cranes are widely used for transporting containers from container ships to trucks. However, there is a residual sway motion of the crane system at the end of the acceleration and deceleration period or in case of unexpected disturbance. In crane systems, trolley motion control is a well-known technique for the suppression of undesirable sway motion [4, 5]. Nevertheless, there are considerable problems with this system, such as increased fatigue and discomfort of crane drivers who work for a long time. As a useful approach towards solving these problems, we intro-

[†] This paper was recommended for publication in revised form by Associate Editor Kyongsu Yi

*Corresponding author. Tel.: +82 51 629 6197, Fax.: +82 51 629 6186

E-mail address: kpjiwoo@pknu.ac.kr

© KSME & Springer 2009

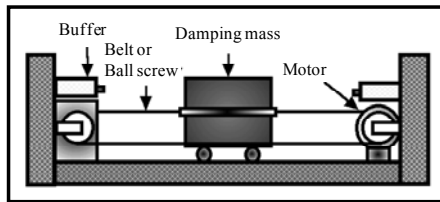


Fig. 1. Actuator for mass damper type anti-sway system [6-9].

duced a new solution [6-9], as illustrated in Fig. 1. The system is referred to as a mass damper type anti-sway system which is installed on the spreader of the crane to suppress undesirable sway motion. The proposed system consists of a damping mass, a belt or a ball screw used for transferring power to the moving mass and a motor which moves the damping mass. In this system, the actuator acting on the auxiliary mass applies inertial control force to the crane system in order to reduce undesirable sway motion.

In real operating environments, processes such as load hoisting and the travel of the trolley involve various complex motions. It is also not trivial to perform precise measurements of such dynamic motions of the crane. Considering real operation conditions, laser sensing systems or camera-based sensing systems have been used as parts of the solution to this problem. However, the applied sensing systems are not useful for actual operation due to their complexity. In this paper, we introduce a camera-based image sensing system for measuring the dynamic motions of crane spreaders on which only a camera system is installed.

In the proposed sensing system, sway motion is measured by using the ratio of the actual distance between two landmarks mounted on the spreader to the distance in the captured image. In this system, the image processing technique used for detecting the landmarks is a kind of robust template matching method vector code correlation (VCC) [16]. On the basis of the experimental results, the usefulness and effectiveness combined with excellent control performance of the proposed image sensing system is demonstrated.

2. System description

As mentioned above, the considered anti-sway system is mounted on the spreader of the crane. As shown in Fig. 2, the anti-sway system is composed of measurement and control parts. The control part,

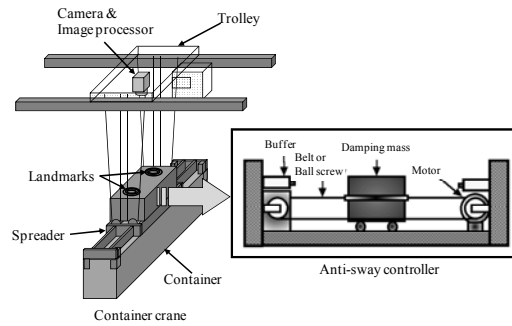


Fig. 2. Schematic diagram of the proposed anti-sway system with a moving mass and an image sensor.

which suppresses undesirable sway motion, is of the mass damper type, and the measurement part is a camera-based image sensing system. To measure the motion, an image sensor with a CCD camera and an image processor is installed on the side of the trolley.

Naturally, it is considered that the anti-sway system should be designed on the basis of information regarding the size, the weight and other parameters of the cargo. In the considered system, it is necessary to install a damping mass, a motor for moving the damping mass, a belt or a ball screw for transferring power to the moving mass and a displacement sensor for measuring the dynamic position of the damper mass [6]. In addition, in the image sensing system, two landmarks are used for measuring the displacement of sway motion.

3. Measurement of sway motion and rope length using the image sensor

3.1 Principle of measuring sway motion and rope length

First, we describe the principle behind measuring sway motion. The measurement of sway motion is equivalent to measuring the displacement of the container spreader as shown in Fig. 3, where (a) and (b) illustrate the anti-sway system in which an image sensor is installed, where the position (X_s, Y_s) illustrates the displacement of the container spreader when it is moved from the origin O_s , corresponding to a static position. This displacement is measured with the image sensor, which is installed on the side of the trolley, after which the center o_c of the image is captured, where o_c corresponds to the center O_s of the spreader in static position. The image sensor detects the positions (x_1, y_1) and (x_2, y_2) of the two landmarks

on the captured image. If these landmarks are used, the change of the height of the spreader caused by the winding and unwinding of the rope can also be measured. Next, the sway motion can be measured by using the ratio of the actual distance D between the landmarks and the distance d on the image. By using the positions of the landmarks, the distance d and the displacement of the spreader in the image, which is defined as (x_s, y_s) , can be calculated as follows.

$$d = \sqrt{(x_1 - x_2)^2 + (y_1 - y_2)^2} \tag{1}$$

$$(x_s, y_s) = \left(\frac{x_1 + x_2}{2}, \frac{y_1 + y_2}{2} \right) \tag{2}$$

If (x_s, y_s) is used, the actual displacement of the spreader is calculated as follows.

$$(X_s, Y_s) = \left(\frac{D}{d} x_s, \frac{D}{d} y_s \right) \tag{3}$$

Here, we will describe the method used for measuring the rope length. The rope length Z_s is divided into two parts (Z_m and Z_c) as shown in Fig. 3 (c), where Z_m is the distance between the origin O_s and the focal point of the image sensor, which is taken from the specifications of the image sensor, and Z_c is the distance between the focal point and the upper surface of the spreader, which is calculated by using the ratio of D and d . If these values are used, the parameter Z_s can be calculated as follows.

$$Z_s = Z_m + Z_c \tag{4}$$

$$Z_c = \frac{D}{d} f \tag{5}$$

3.2 Detection of the landmarks by using the Vector Code Correlation (VCC)

The template matching method detects a target by scanning the entire image, while comparing a partial image of the same size with a template containing the target. Here, we apply this method to the image sensor for detecting the landmarks. In general, the time needed for processing the captured image is long, although it depends on processor performance and algorithms for the template matching. Thus, we apply an improved template matching method referred to as vector code correlation (VCC) for detecting the landmarks. In the VCC method, the gradient calcu-

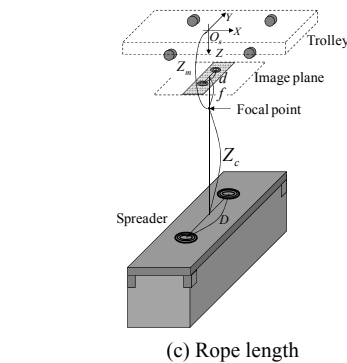
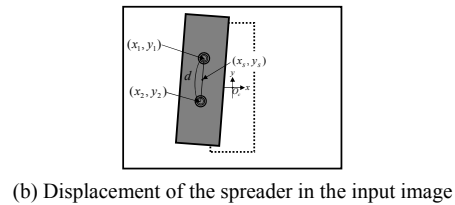
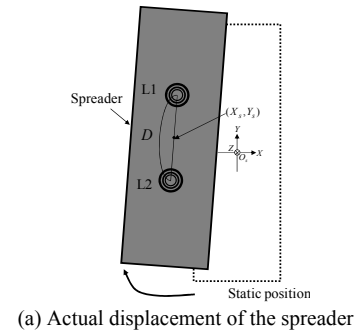


Fig. 3. Principle of measurement of sway motion and rope length by using an image sensor.

lated by using the intensity of eight neighboring pixels for each pixel is coded, and the general scheme of the VCC is shown in Fig. 4. The vertical and the horizontal gradient of the intensity for each pixel are coded by a vector code with two bits. The gradient of a vector code has three values: 01 (positive), 00 (near zero), and 10 (negative) for each direction. Since two gradients exist for each pixel, the information of a vector code image is represented with four bits per pixel. The matching of the VCC is easily performed by counting the equivalence with an XOR operation between the input image and the template coded by the vector code. Due to these features, the VCC method can reduce the processing cost and can improve the robustness against light fluctuations under dynamical outdoor conditions where container cranes are operated.

3.3 Countermeasures against changes in the height of the spreader

A template including a landmark is a partial image captured at a certain height. Since the size and the shape of the landmark change in accordance with the height of the spreader, the matching of the template with a partial image, including the landmark, might fail. To overcome this problem, we adopted two countermeasures involving the shape of a landmark and the replacement of the template.

(1) Shape of landmarks

To adjust the template to the changes in the height of a spreader in the image sensor, we employed a landmark which has similar appearance at different heights. Fig. 5 shows the landmark consisting of concentric circles, where the width of the line is changed by a certain ratio. The diameter and the line width of the largest circle in Fig. 5(a) are 50 and 5.3mm, respectively, while those of the second and the third circle become smaller by a ratio of 0.7. Although the size of the landmark in the image changes in accordance with the changes in the height of the spreader, the central portion of the landmark remains almost the same, regardless of its size, as shown in the rectangles in Fig. 5(a) and (b). Therefore, a landmark composed of concentric circles is useful as a template which is robust against changes in size, and has the advantage of being easy to find and match in the images on the sensor. However, to account for the case where the landmark is not found in the image, which occurs when the color of the line of the outermost circle changes at a certain height (for example, as shown in Fig. 5(c) in comparison to the standard template in Fig. 5(a)), we adopted the template replacement method.

(2) Template replacement

This is a method for replacing the current template

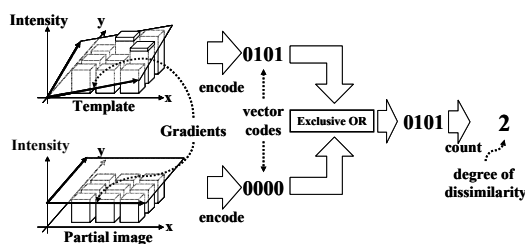


Fig. 4. Scheme of the vector code correlation method.

with a new one if the similarity between the standard template and the template detected from an image is higher than a certain level. In concrete terms, as shown in Fig. 6, the landmark is found in the detected image extracted by matching the current template with a partial image in the input image (Fig. 6(a)). Subsequently, it is ensured that the detected image is identical to the provided standard template by comparing the two images (Fig. 6(b)). Here, using the standard template prevents the current template from being replaced with the detected image if the latter includes a different object. If the value resulting from the comparison is higher than a certain threshold (Fig. 6(c)), the current template is replaced with the detected image (Fig. 6(d)). Otherwise, the current template remains unchanged. Since the new template becomes more similar to the landmark captured at a different height than the standard one, the image sensor can detect the landmark for the entire range of heights of the spreader.

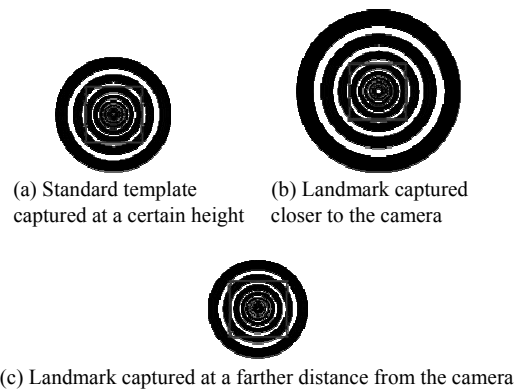


Fig. 5. Landmarks consisting of concentric circles whose line width changes by a certain ratio.

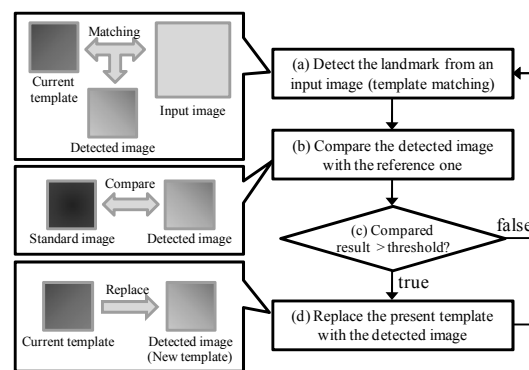


Fig. 6. Processing flow for rule-based template replacement.

4. Description of anti-sway system

The trolley control technique is well known and commonly used for suppressing undesirable sway motion. In addition, a large number of recent studies have proposed the realization of typical anti-sway trajectory control for experienced operators based on techniques such as high hoisting. However, the high hoisting technique is not useful for container crane systems. Also, the trolley control strategy is prone to various problems, such as increased fatigue and discomfort of crane operators who work continuously for long periods of time. To resolve these problems, we introduced a new solution as illustrated in Figs. 1 and 2 [6-9]. If the proposed mechanism is installed on the spreader of the crane, undesirable sway motion can be effectively suppressed.

Fig. 7 shows a dynamic model where the container crane is taken as the controlled system. In this system, we assume that θ is small and the spreader makes a leveling movement, in other words, $x=l\theta$. These facts indicate that a linearized model can be derived. As a result, the system can be described in the following way [6-9].

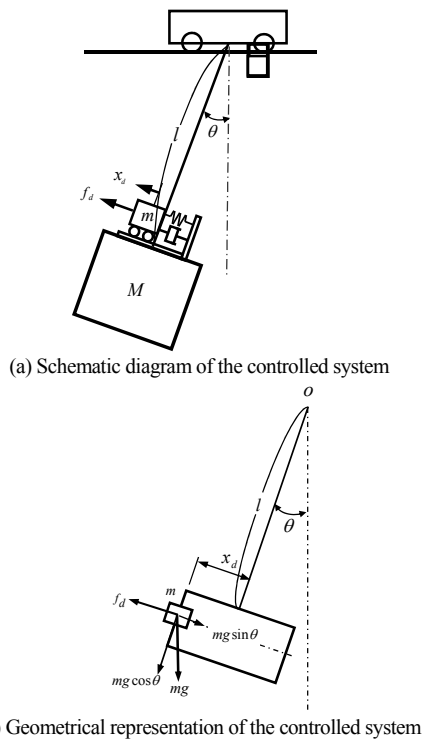


Fig. 7. Dynamic model of the controlled system.

$$(M + m)\ddot{x} + \frac{C}{l}\dot{x} + (M + m)gx = T - mgx_d - f_d l \quad (6)$$

$$m\ddot{x}_d = -\frac{mg}{l}x + f_d - C_d\dot{x}_d - k_d x_d \quad (7)$$

Here, C is the damping constant, T is the moment generated by disturbance, $f_d=k_m i$ (k_m : torque constant, i : motor current) is the horizontal force generated by the actuator, C_d is the damping constant and k_d is the stiffness of the actuator. In this case, the equation of state for the overall system is given by

$$\begin{aligned} \dot{x}_p &= Ax_p + Bu + Dw \\ y &= Cx_p \end{aligned} \quad (8)$$

where the states $x_p = [x \ \dot{x} \ x_d \ \dot{x}_d]^T$, $u=v$ (input voltage to motor), $w=T$ (disturbance input).

Here, we have designed a controller on the basis of the H_∞ control approach, which is robust to system uncertainties and unexpected disturbances [10-13]. In other words, the designed controller governed by the following Eq. (9) satisfies the norm condition $\|Z\|_\infty < \gamma$ (>0), where Z is the transfer function of the disturbance input w to the controlled output x . Therefore, the controller is calculated as follows:

$$K(s) := \begin{bmatrix} A_c & B_c \\ C_c & D_c \end{bmatrix} \quad (9)$$

where,

$$\begin{aligned} A_c &= \begin{bmatrix} -2.5234 & -0.5709 & -0.4550 & -2.4035 \\ 0.5100 & -4.3636 & -2.2421 & 1.3109 \\ -4.5748 & 5.0089 & -10.1794 & -3.2709 \\ -7.5437 & -3.4879 & -21.4871 & -43.4999 \end{bmatrix}, \\ B_c &= \begin{bmatrix} 0.8803 & -2.1623 \\ -13.7120 & -1.0277 \\ 12.2821 & -3.1357 \\ 4.8467 & -4.5473 \end{bmatrix}, \\ C_c &= [0.0602 \ 0.0658 \ 0.1519 \ -0.642], \\ D_c &= [0 \ 0] \end{aligned} \quad (10)$$

5. Experiment

To demonstrate the usefulness of the proposed anti-sway system with an image sensor, we performed an experiment using the pilot model of a crane as shown in Fig. 8. The crane model is composed of a trolley

Table 1. Parameters for control system design.

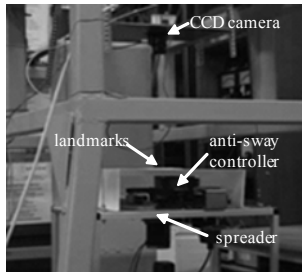
Parameters	Values
C	0.005324 [N·s/m]
C_d	1.586 [N·s/m]
k_d	0.00095 [N/m]
k_m	9.88 [N/A]
M	0.565 [kg]
m	0.095 [kg]
g	9.8 [m/s ²]

Table 2. Parameters for control system design.

Camera	PX-VGA120-LM (Mono)
Resolution	640×480 [pixel]
Pixel size	7.4×7.4 [μm]
Focal length	12 [mm]
Largest circle diameter	50mm
Largest circle line width	5.3mm
Ratio of circles	0.7
Distance between landmarks	70 [mm]
Processing speed	110 [fps]



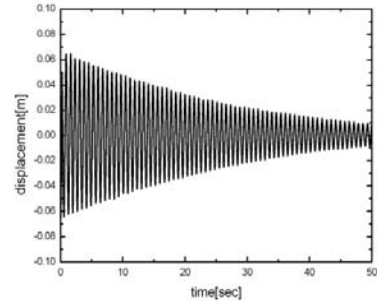
(a) Anti-sway system for container cranes



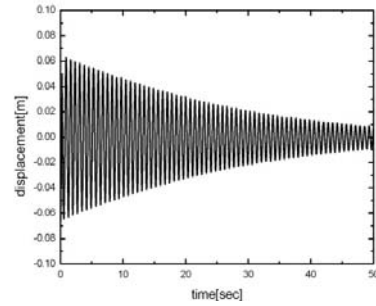
(b) Measurement system with image sensor

Fig. 8. Crane model equipped with the proposed anti-sway system.

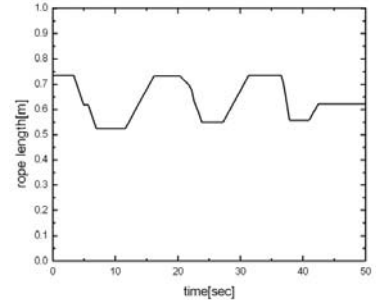
and a mass damper type anti-sway system. The anti-sway system is installed on the spreader to suppress the sway motion caused by the moving trolley, load hoisting and unexpected disturbances. This new approach utilizes a scheme which is different from that



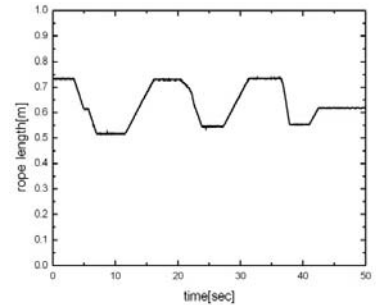
(a) Sway motion as measured with a laser sensor



(b) Sway motion as measured with an image sensor



(c) Changes of rope length as measured with the encoder



(d) Changes of rope length as measured with the image sensor

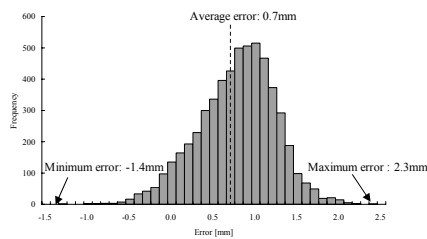
Fig. 9. Comparison of the results obtained with the two sensing systems.

of typical anti-sway systems [1-5, 14, 15]. In the proposed system described above, the image sensor is used as the measurement system. It is composed of a camera installed on the side of the trolley and two

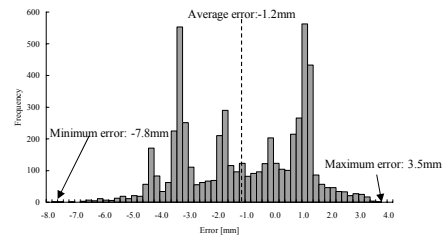
landmarks on the spreader part, as shown in Fig. 8(b). This sensing system can simultaneously measure changes in both the displacement and the height of the spreader. The parameters for the control system design and the characteristics of each sensor are listed in Tables 1 and 2

First, we present the measurement results in order to verify the usefulness of the image sensing system. The results of a comparison between the image sensing system and other systems are illustrated in Fig. 9, where (a) and (b) show the sway motion of the spreader as measured with the laser sensor and the image sensor, where the hoisting length of the rope is 430mm. Furthermore, (c) and (d) show the changes in

the hoisting length (rope length) as measured with the encoder and the image sensor, respectively. Naturally, the changes in the sway motion and the rope length are measured simultaneously by using the image sensor. These results show that the image sensor can perform continuous measurements without losing sight of the landmarks. In addition, to evaluate the measurement accuracy of the image sensor, in Fig. 10 we show the frequency distributions of the measurement errors between the image sensor and other sensors, where (a) shows the frequency distribution of the measurement error between (a) and (b) in Fig. 9, while (b) in Fig. 10 shows the frequency distribution between (c) and (d) in Fig. 9. In these results, the

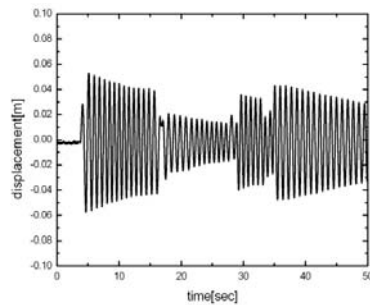


(a) Frequency distribution of measurement errors between Fig. 9(a) and (b)

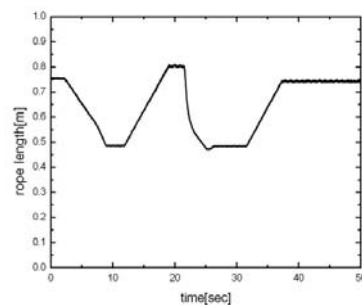


(b) Frequency distribution of measurement errors between Fig. 9(c) and (d)

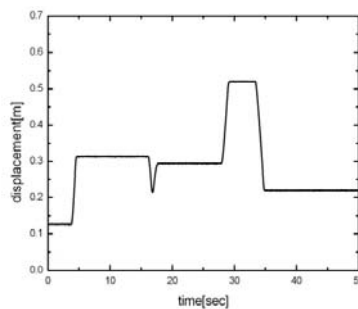
Fig. 10. Frequency distributions of measurement errors between the two sensing systems.



(a) Sway motion of the crane spreader



(b) Changes in rope length



(c) Traveling distance of the trolley

Fig. 11. Response of the system when the load is hoisted and the trolley is traveling (no control system).

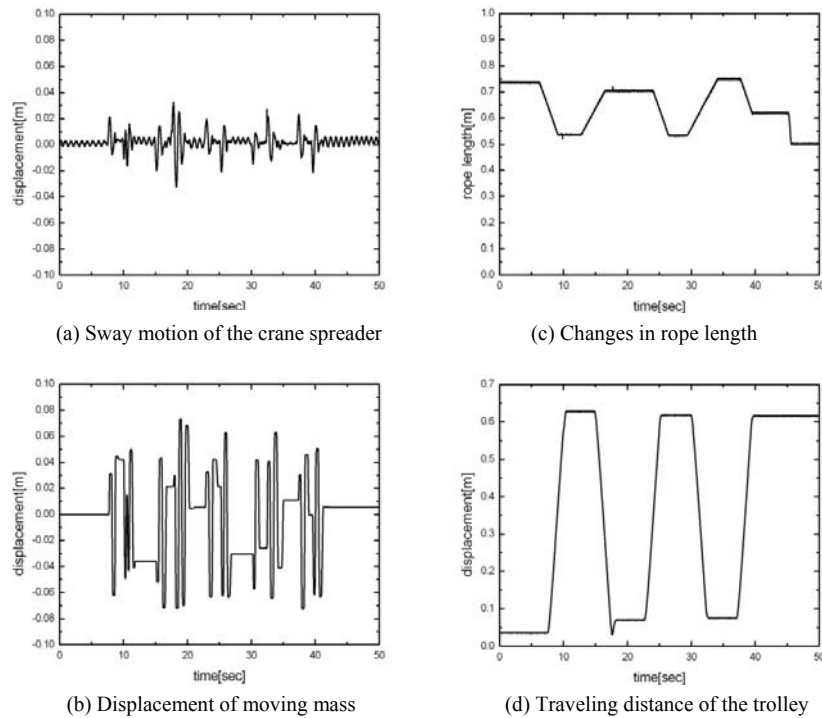


Fig. 12. Responses of the system when the load is hoisted and the trolley is traveling (with the proposed control).

absolute measurement accuracy of the image sensor with respect to the sway motion is $2.3\text{mm}_{\text{max}}$, and the absolute accuracy for the changes of the hoisting length is $7.8\text{mm}_{\text{max}}$. These results show that the proposed image sensing system guarantees accurate control and robust design of the control system.

The performance of the proposed anti-sway system based on an image sensor has been demonstrated with experiments. Fig. 11 shows the response of the system in the case where no control is exerted and while the load is hoisted and the trolley is traveling. The performance of the controlled system under the same conditions is shown in Fig. 12. Specifically, in this figure, (b) shows the dynamics of the actuator in the mass damper type anti-sway system, where the actuator acting on the movable mass applies inertial force to the spreader and which suppresses undesirable sway motion. Comparing the sway motions shown in the respective (a) panels of Figs. 11 and 12, it is clear that the undesirable sway motion shown in Fig. 11 has been effectively suppressed.

6. Conclusion

A new anti-sway control system has been designed

by employing a mass damper type anti-sway technique and an image sensing system. Although laser and ultrasonic sensors are used in typical sensing systems, the presence of several sensors complicates the design of the sensing system and incurs high cost, which can result in lowered system performance. Therefore, an anti-sway control system composed of an anti-sway controller and an image sensor has been proposed in this paper. It has been verified that the proposed sensing system has a sufficiently high measurement accuracy and reliability such that it is applicable to anti-sway system design. In particular, the proposed sensing system can simultaneously measure changes in the displacement and the height of the spreader. This excellent property can promptly find application in industry.

From the obtained experimental results, it is clear that the usefulness of the image sensing system and excellent control performance is guaranteed when the load is hoisted and the trolley is traveling. Moreover, the usefulness of the proposed anti-sway system has been verified, and the possibility that the considered system can be applied in real settings has been confirmed.

References

- [1] T. T. Soong, *Active structural control: Theory and Practice*, Longman Scientific and Technical, Essex, England, (1990).
- [2] Y. Fujino, T. T. Soong and B. F. Spencer Jr, Structural control: Basic concepts and applications, *Proc. of ASCE Struct. Cong. XIV*, Chicago, Illinois, USA (1996) 1277-1287.
- [3] G. W. Housner et al., Structural control: Past Present and Future, *J. of Eng. Mech.*, 123 (6) (1997) 897-971.
- [4] W. Cheng and X. Li, Computer control of high speed cranes, *Proc. of the American Control Conference*, San Francisco, California, USA (1993) 2562-2566.
- [5] N. Nomura, Y. Hakamada and H. Saeki, Anti-sway position control of crane based on acceleration feedback and predicted pattern following method, *Trans. of the Institute of Elec. Eng. of Japan (D)*, 17 (11) (1997) 1341-1347.
- [6] Y. B. Kim, *Anti sway system of the crane*, Korean patent, No. 0350780, (2002).
- [7] G. B. Kang, Y. B. Kim, S. B. An, G. H. Chae and J. H. Yang, A new approach to anti-sway system design for a container crane, *Proc. of the SICE Annual Conference 2003*, Fukui, Japan (2003) 335-339.
- [8] S. B. An, Y. B. Kim, G. B. Kang and G. Zhai, Anti-sway control system design for the container crane, *Proc. of the International Conference on Control, Automation and Systems*, Gyeongju, Korea (2003) 1404-1409.
- [9] Y. B. Kim, M. Ikeda, J. H. Suh, G. Zhai and S. H. Han, Robust control design for the mass-damper type anti-sway system, *Proc. of the SICE-ICCAS International Joint Conference 2006*, Busan, Korea (2006) 4130-4133.
- [10] S. Boyd and L. El. Ghaoui, *Linear Algebra and Its Applications*, SIAM Book, Philadelphia, Pennsylvania, USA (1993) 63-111.
- [11] P. Apkarian and P. Gahinet, A convex characterization of gain-scheduled H_∞ controller, *IEEE Trans. AC*, 40 (5) (1985) 853-865.
- [12] A. Packard, Gain scheduling via linear fractional transformations, *System & Control Letter*, 22 (2) (1994) 79-92.
- [13] R. E. Skelton, T. Iwasaki and K. M. Grigoriadis, *A unified algebraic approach to linear control design*, Taylor & Francis, London, England (1998).
- [14] T. Chikura, M. Yamamoto, T. Monzen and K. Uchida, Development of automated transfer crane in a port container yard, *JSME Trans. C (in Japanese)*, 71 (4) (2005) 213-218.
- [15] Automatic, remotely controllable transfer crane, *Mitsubishi Heavy Industries Technical Review*, 44 (2) (2007) 21.
- [16] D. Koyama, Y. Choi, T. Iyota and Y. Kubota, A technique of high-speed template matching using vector code correlation, *Proc. of the JACC (in Japanese)*, Okayama, Japan (2003) 785-788.



Hideki Kawai received his B. S. and M. S. in Information Systems Science from Soka University, Japan, in 2004 and 2006, respectively. He is currently a doctoral student at Soka University. His research interests include robust image processing and image sensing system design.



Yong Woon Choi received his M. S. degree in System Engineering from Kobe University, Japan, in 1990. He then received his Ph. D. in System Science from Kobe University, in 1995. Dr. Choi is currently an Associate Professor at the Faculty of Engineering at Soka University in Tokyo, Japan. His research interests include robot vision and robot navigation control.



Young Bok Kim received his B.S. and M.S. in Maritime Engineering from National Fisheries University of Busan, Korea, in 1989 and 1991, respectively. He then received his Ph.D. from Kobe University, Japan in 1996. Dr. Kim is currently a Professor at the School of Mechanical Engineering at Pukyong National University in Busan, Korea. His research interests include control theory and application with dynamic ship positioning and crane control system design.